10.22059/IJVM.2022.331329.1005197

Iranian Journal of Veterinary Medicine
Volume 16- Issue 3

Case Report

Online ISSN: 2252-0554

Feasiability of Using Evidence-Based Virtopsy to Answer the Possible Clinical and Post-Mortem Questions, in Veterinary Practice

Mohammad Molazem[1,2]*, Arezoo Ramezani[1], Sarang Soroori[1], Zahra Jafari Giv[1], Sara Shokrpoor[2], Urs Geissbuehler[3]

1. *Department of Surgery and Radiology, Faculty of Veterinary Medicine, University of Tehran, Tehran, Iran*
2. *Department of Pathology, Faculty of Veterinary Medicine, University of Tehran, Tehran, Iran*
3. *Department of Clinical Veterinary Medicine, Division of Clinical Radiology, Vetsuisse Faculty of Bern, University of Bern, Bern, Switzerland*

Abstract

A post-mortem examination is an important part of evidence-based medicine to understand the deterioration of clinical signs or causes of death in euthanized or deceased individual animals or even populations.

Post-mortem analysis is aimed at improving clinical treatment and therapy, confirming a suspected diagnosis, managing breeding strategies, and clarifying the forensic cases (e.g., neglect or animal abuse). In analogy to virtopsy in human medicine, diagnostic imaging modalities have been applied in post-mortem veterinary medicine, which we call vetvirtopsy.

We hypothesize that vetvirtopsy can be used as a method to answer certain clinical/post-mortem questions to improve the diagnosis reliability. In some questions, vetvirtopsy actually can replace conventional necropsy. This overview study aims to compare vetvirtopsy with conventional necropsy for variable causes of death in animals and to define its possibilities and limitations.

Deceased or euthanized pets and wild animals were collected. The imaging techniques, such as post-mortem digital radiography, post-mortem ultrasound, post-mortem computed tomography, and post-mortem magnetic resonance tomography combined with image-guided tissue sampling, were used to address the open questions about clinical symptoms or causes of their death.

The case series in this project showed that diagnostic imaging techniques are feasible in answering distinct ante-mortem and post-mortem clinical and forensic questions. However, there is an interdisciplinary collaboration between diagnostic imaging and sampling under imaging guidance.

KEYWORDS: Computed tomography, Magnetic resonance tomography, Radiography, Ultrasound, Virtopsy

Correspondence

Mohammad Molazem, Department of surgery and radiology, Faculty of veterinary medicine, university of Tehran, Tehran, Iran. Tel: +98(21) 61117149, Email: Mmolazem@ut.ac.ir

Received: 2022-01-03

Accepted: 2022-03-14

How to Cite This Article
Molazem, M ., Ramezani, A., Soroori, S, Jafari Giv, Z, et al. (2022). Feasiability of Using Evidence-Based Virtopsy to Answer the Possible Clinical and Post-Mortem Questions, in Veterinary Practice. *Iranian Journal of Veterinary Medicine, 16*(3), 311-337.

Introduction

A post-mortem examination is an important technique in veterinary evidence-based medicine to identify the causes of death and improve medical treatment or breeding strategies. In some cases, such as animal abuse, neglect, or suffering, the post-mortem examination also has forensic value (Benetato *et al.*, 2011; Watson *et al.*, 2017). In addition, it is useful for confirming a suspected disease in poor prognostic cases with several differential diagnoses, in cases of limited economic owner possibilities, unknown history, and in forensic cases (e.g., animal protection). Although autopsy is the current standard in veterinary medicine (Hostettler *et al.*, 2015), the number of conventional necropsies at the Institute of Veterinary Pathology, Vetsuisse Faculty, Zurich, Switzerland, decreased markedly in the recent years. The annual average of conventional necropsies during 2010-2013 was 350 dogs and cats. It has been reported that 300 dogs and cats in 2014 and only 151 cases in 2015 (until 26.11.15) underwent conventional necropsy (Pewsner *et al.*, 2017).

In recent years, respect for and ethical values of pets continuously increases in a humanistic view of the world. In today's society, the position of animals is changing more and more to social partners and family members. In addition, religious reasons could also explain the reduction in conventional necropsies (Thali *et al.*, 2009). In human forensic medicine, cross-sectional imaging techniques, such as post-mortem computed tomography (CT), post-mortem magnetic resonance imaging (MRI), photogrammetry-based three-dimensional (3D) optical surface scanning, CT-guided biopsies, and minimally invasive CT- or MR- angiography are used regularly to complement or replace autopsy (Thali *et al.*, 2007). Literature comparing 2D and 3D post-mortem imaging procedures and conventional necropsies in veterinary medicine are very rare (Ibrahim *et al.*, 2012).

The term "virtopsy" is a compound of the words "virtual" and "autopsy". In this context, virtual means *artificial and produced by a computer*. An autopsy is a combination of the Greek words "utos" for *self* and "psomei," for *I will see*. Therefore, an autopsy means "*to see with one's own eyes*" (Ibrahim *et al.*, 2012). The process of an autopsy is an unrepeatable, operator depending act (Thali *et al.*, 2010). Consequently, non-obvious or unexpected findings can be lost in the external examination. Such findings might include small fractures, pathologic gas, fluid accumulations, relevant thrombi, and decent soft tissue trauma.

The use of virtopsy in veterinary medicine was very limited until 2004 and was often used for diagnosis confirmation (Buck *et al.*, 2009; Delannoy *et al.*, 2012). However, in recent years, studies have shown that virtopsy, especially in small animals, is an efficient method to prevent necropsy and save time, resources, and energy (Ibrahim *et al.*, 2012). Therefore, the present study aimed to prove the essential role of virtopsy in the question-based determination of dead animals. For this purpose, a case series of virtopsy is presented in routine veterinary practice to demonstrate its potential use for different clinical or forensic questions.

Materials and Methods

The study population consisted of deceased or euthanized pets and wild animals which were referred to the Small Animal Hospital of the University of Bern and the Small Animal Hospital of the University of Tehran during 2017-2020. While the authorities requested wild animal post-mortem examination, the request for pet post-mortem animals was rooted in medical interest. For all pets, post-mortem examination consent was obtained from the owners. History, time of death or euthanasia, and open questions about clinical symptoms or the causes of death were recorded in a survey sheet for each case prior to the imaging examination.

Based on this information, the cases were categorized into three groups to find out whether it is possible to detect the cause leading to prognostically hopeless clinical signs in pets. This question is frequently asked in research autopsy with the primary goal of collecting tissue to support basic or translational research. This approach has increasingly been used to investigate the pathophysiological mechanisms of cancer evolution, metastasis, distribution, and treatment resistance (Watson *et al.*, 2017). In the second group, we were interested in detecting the cause of death in dead found animals. Owners, clinicians, and authorities may oppose an autopsy for a variety of reasons, including the fear of animal abuse or suffering and for taking care of the animals in danger of extinction. In the third group of cases, we aimed to understand if it is possible to identify the animal and the probable cause of dead bog bodies.

A non-destructive method enables the gentle examination of fragile bog bodies. Based on open questions, the cadavers underwent an examination of one or several regions of interest or whole-body imaging by choosing one or some of the following diagnostic imaging modalities. Radiographs were performed with a direct digital radiography (Kodak casestream directview classic) or computed digital radiography (Fuji smart CR-XG-[1]) systems. CT was either conducted with a 16-slice (Philips Brilliance 16, Netherland) or a 2-slice (Siemens Somatom, Germany) helical machine. The selection of slice thickness depended on the body weight and measured 1.5 2.5 and 3 mm in body weights of 1-10, 10-30, and 30-60 kg, respectively. MRI was performed with a 1.0 Tesla device (Philips panorama, 1.0 T, HFO, Netherland). STIR sequences were completed in the region of interest.

Possible examination areas in CT and MRI were "head, neck and front limbs," "thorax," and "abdomen and hind limbs" The decision for ultrasound or CT-guided tissue biopsies was based on open questions and imaging findings and was assessed by the Institute of Veterinary Pathology of the University of Bern or by the Department of Veterinary Pathology of the University of Tehran. Imaging findings were analyzed based on the ability to answer the clinical questions about the patient.

Results

During a period of 6 years, from 2014 to 2020, a virtopsy was performed on 20 carcasses of 12 animal species of different ages and genders (Table 1). The protocols included 11 whole-body and partial CT scans, four partial MRI examinations, one ultrasonography, four ultrasound-guided samplings, and 18 radiographs (Table 1). Neoplasia (N=3), infection (N=3), trauma (N=8), and hallow organ rupture (N=2) were the fetal pathologies noted in this study (Table 1). Six cases were assigned to the first group, in which virtopsy could figure out the cause of hopeless clinical signs by the following necropsy confirmations.

Case no. 1

A seven-year-old flat-coated retriever female dog was evaluated for her inability to chew and pain when chewing. In addition, recurrent ear infections occurred shortly after starting the treatment. The exact location of the pain was not recognizable. The animal was euthanized due to the poor quality of life and prognosis. The owner gave consent for a postmortem examination. An hour after death, in postmortem latero-lateral radiography of the skull, a decent, round, granular soft to the opaque mineral lesion was observed caudal to the bullae, partly superimposed to the nasopharynx and retropharyngeal soft tissues (Figure 1).

In CT scan, a monostotic aggressive bone lesion of the left condylar process mainly affecting the mandibular fossa with soft tissue mineralization and otitis media was detected. Differentials included neoplasia and osteomyelitis (Figure 2). Subsequently, CT-guided bone biopsy (2×) using a bone marrow biopsy set 11 G×100 mm from the left mandibular condyle was performed for histopathologic examination. In a histopathological specimen study, osteosarcoma was confirmed.

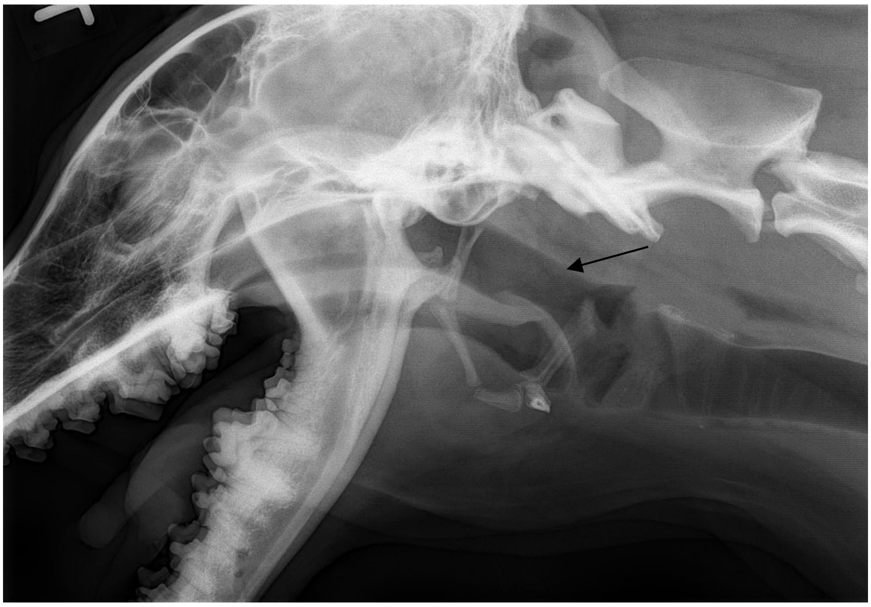

Figure 1. Post mortem LL radiography of the skull of a 7-year-old Flat-coated retriever female dog. An ill-defined decent soft tissue to the opaque mineral lesion was seen caudal to the tympanic bullae (Black arrow).

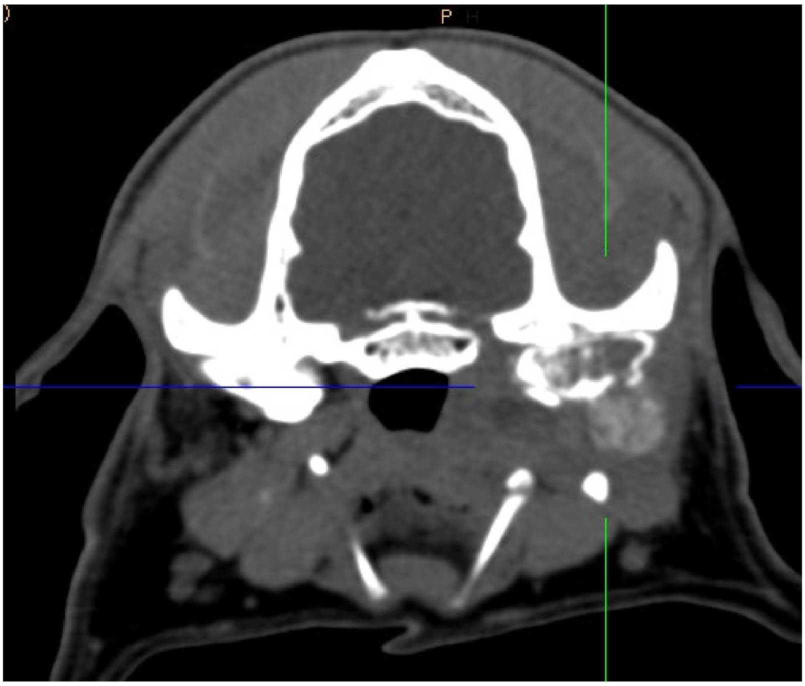

Figure 2. Transverse CT image of the temporomandibular joints of case 1: aggressive bone lesion of the left condylar process with granular-like mineralization ventral. The soft tissues of this area are increased, and the left lateral aspect of the nasopharynx is flattened

Case no. 2

An eleven-year-old male Persian cat was presented with a history of chronic cough and right forelimb lameness for one week. Regarding age and financial limits, the animal was euthanized at the request of the owner. No palpatory lesion could be found in the gross examination. Post-mortem MRI and CT imaging were performed to assess if a lesion existed at the right forelimb and if there were signs of metastases.

In whole-body CT, a large mass in the right supraspinatus muscle with predominantly proliferative bone changes in the scapula and enlargement of the right ipsilateral axillary lymph node were detected (Figure 3). On whole-body MRI (STIR) examination, soft tissue lesions were identified in the right forelimb, left and right hindlimbs, as well as left pectoral, right epaxial, and left gluteal muscles. Consolidation of the entire left lung lobes was also visible (Figure 4). An ultrasound-guided biopsy was performed for the lung lesion, which turned out to be a mast cell carcinoma (solid carcinoma). However, the affected tissue could not be assessed by biopsy and might be intercostal or diaphragmatic muscles.

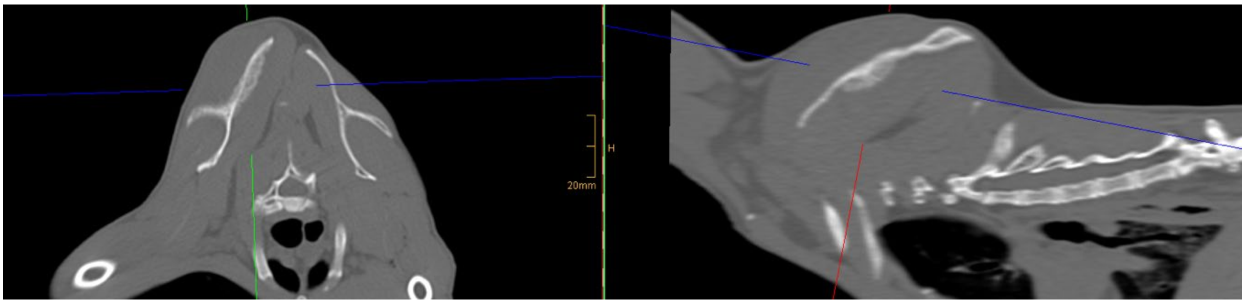

Figure 3. Transverse and parasagittal post mortem CT-images of an 11-year-old male Persian cat at the level of the right scapula, bone window; predominantly proliferative bone lesion of the right scapula.

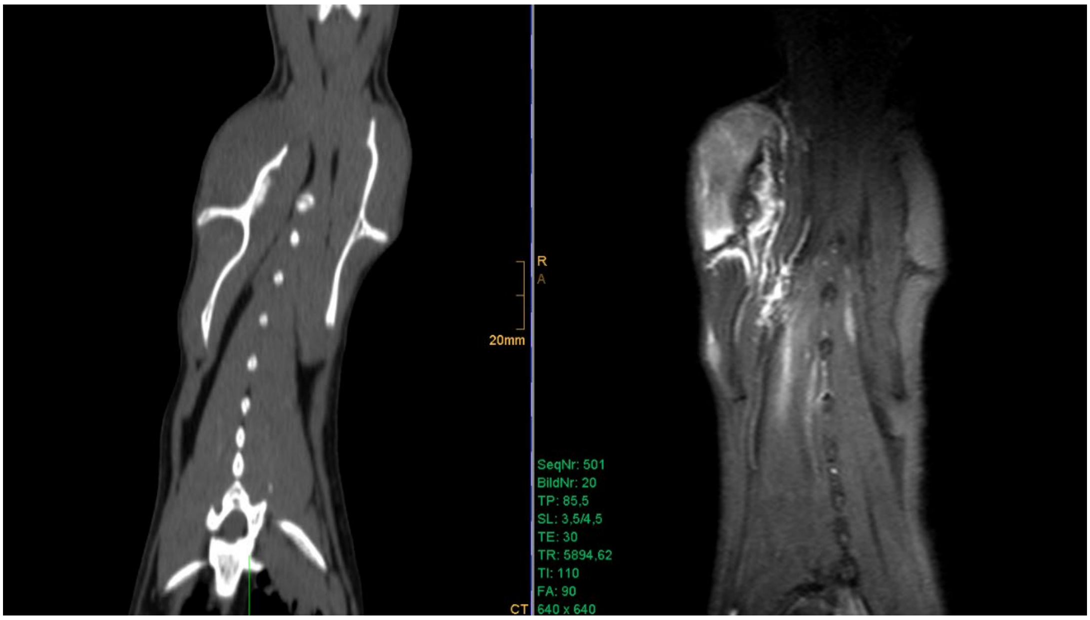

Figure 4. Dorsal post-mortem CT reconstruction image (left side) and dorsal MRI SPIR image of the right scapular region of the same case in Figure 3 show proliferative scapular changes and marked heterogeneous hyperintensity in the supra- and infraspinatus muscle.

Case no. 3

A sixteen-year-old female cat with a history of anorexia, epileptic seizures, ataxia, and vomiting presented with a heart murmur and abdominal tenderness in clinical examination. She was euthanized due to a poor prognosis. Post-mortem left lateral and ventrodorsal (VD) radiographs of the chest were performed immediately after euthanasia to further examine the thorax. A large thoracic volume with gas accumulation in the esophagus and stomach and diffuse bronchointerstitial lung pattern with soft tissue opacity of the right middle lung lobe was detected. The lung changes were most likely consistent with allergic bronchitis, such as feline asthma (Figure 5).

A post-mortem sagittal MRI STIR sequence of the cervical, thoracic, and lumbar spine and a transverse SPIR sequence of the lumbosacral junction were performed. The signal intensity increased in the left humerus (Figure 6), paravertebral muscles, left and right lateral soft tissues of L7, and the ventral aspect of the vertebral canal of the L7. Post-mortem abdominal ultrasonography showed generalized small intestinal muscular layer thickening up to 1.5 mm (Figure 7). Ultrasound-guided fine-needle aspirates of the small intestinal muscularis confirmed high-grade lymphoma. Therefore, the antemortem clinical signs were most likely due to the multicentric distribution of neoplasia.

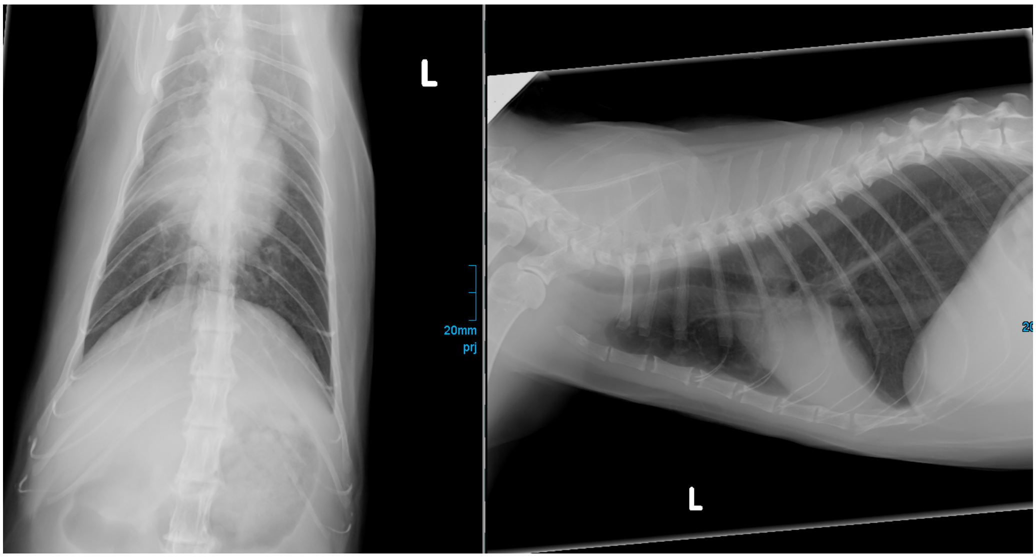

Figure 5. Immediate post-mortem radiographs of a sixteen-year-old female cat show a large thoracic volume with considerable gas in the stomach and a diffuse bronchointerstitial lung pattern. The right middle lung lobe is soft tissue opaque (consolidation)

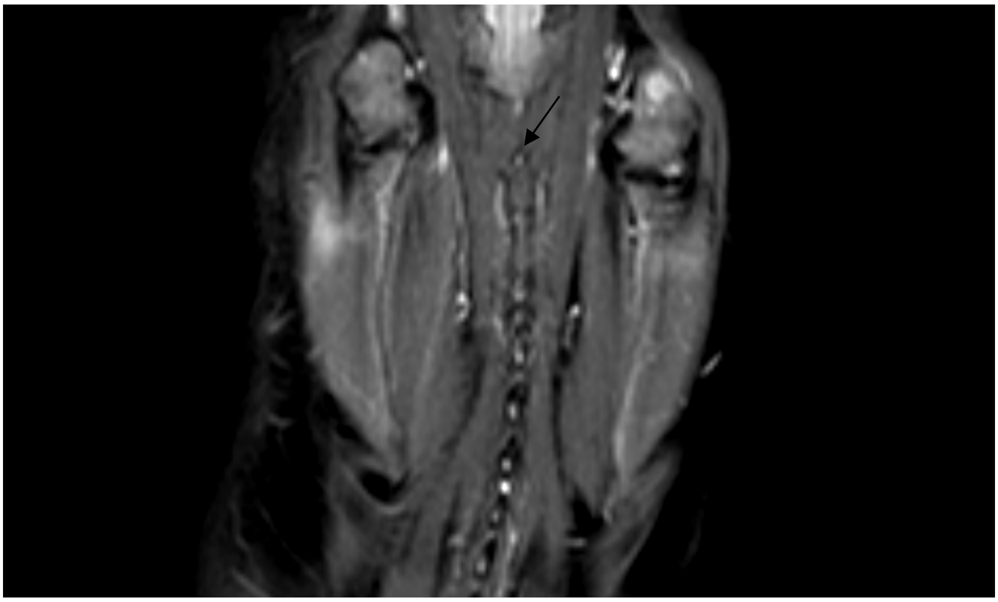

Figure 6. Focal STIR hyperintensity of the same case as Fig 5 in the left proximal humerus metaphysis in a dorsal MRI image (arrow).

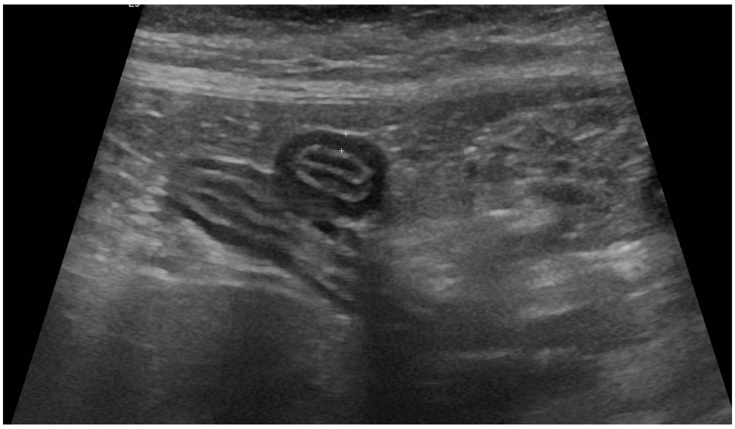

Figure 7. Transabdominal post-mortem ultrasound with a linear probe demonstrates concentric muscular thickening in two jejunal loops.

Case no. 4

A recently deceased six-year-old African grey parrot of unknown gender was referred with a history of chronic apathy and anorexia. The bird died during a clinical examination. In clinical post-mortem examination, a mass was observed between the mandibles. The owner requested a virtopsy to obtain further information about the cause of death. Lateral and VD radiographic projections of the whole body were taken. A space-occupying soft tissue lesion was observed caudal to the beak. Furthermore, a large volume of gas was found in the intestines, which could be a post-mortem change.

CT scans of the skull performed almost 4 h post-mortem revealed a well-defined homogeneous soft-tissue attenuating (HU=12) mass, which was visible at the ventroproximal aspect of the trachea, narrowing its lumen. At the same level, an additional irregular soft-tissue attenuating mass was visible in the dorsal wall of the trachea. Both lesions partially obstructed the upper airway tract (Figure 8). Ultrasound-guided fine-needle aspiration of the ventral tracheal lesion was performed. Cytological examination revealed an abscess. A focused necropsy at the area of the mass confirmed the findings.

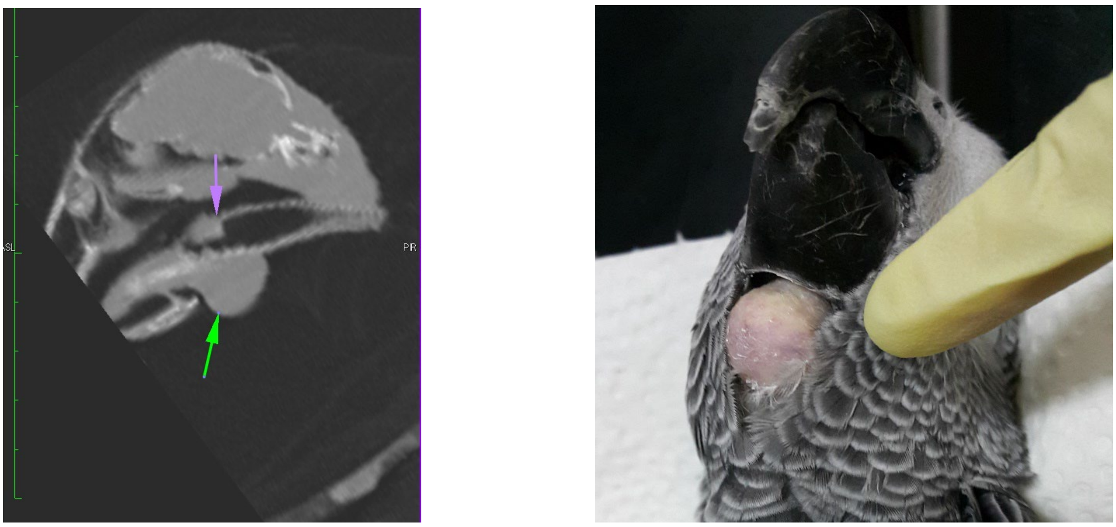

Figure 8. Reconstructed sagittal CT image (bone window) and photograph of a six-year-old African grey parrot of anonymous sex in the skull region showing a homogeneous soft tissue attenuating mass ventral to the ventral and in the dorsal tracheal wall (arrows).

Case no. 5

A twelve-year-old euthanized male mixed breed dog with a history of chronic bilateral forelimb lameness was referred for virtopsy to verify the suspicion of leishmaniosis. Post-mortem lateral and cranio-caudal radiographs of both stifles were performed. On the images of the right stifle, there was a smooth periosteal reaction on the distal metaphysis of the femur, along with the inhomogeneous moth-eaten lysis and patchy sclerosis of the cancellous bone of the distal metaphysis of the femur and the proximal metaphysis of the tibia. The bone cortex was interrupted, and a bone defect was also visible at the distal end of the patella. Multiple small subcutaneous gas opacities were delineated in the lateral aspect of the distal part of the femur.

The lytic changes in the left stifle were significantly less pronounced, and the periosteal changes and gas opacities were not visible (Figure 9). The differential diagnosis of the aggressive bone lesion in the distal femur and proximal tibia were more likely related to fungal osteomyelitis, and neoplasia was unlikely. Bone biopsy was performed under ultrasound guidance. Histopathological evaluations detected multifocal osteolysis by osteoclasts with the fibrosis of the bone tissue, and multifocal infiltrates with macrophages, lymphocytes, and isolated polygonal cells. These findings were compatible with an inflammatory process with remarkable bone resorption. Biopsy of the bones confirmed Leishmania infection.

Figure 9. Bilateral aggressive bone lesions in the distal femurs and proximal tibiae of a 12-year-old euthanized male mixed breed dog

Case no. 6

A seven-month-old female pig was referred with tetraplegia. On neurological examinations, the myelopathy of C6 to T2 and pain in the neck were observed. The animal was euthanized with the consent of her owner. The carcass of the animal was subjected to post-mortem imaging studies to determine the cause of the neurological complication.

According to the history, lateral radiographs of the cervical vertebrae were taken. The body of C7 was shortened with the narrowing of the intervertebral disc space of C6/C7 and focal dorsoventral narrowing of the trachea at the thoracic inlet associated with moderate ill-defined increased ventral soft tissue swelling that minimally compresses the dorsal trachea lumen (Figure 10). The findings were consistent with a collapse of C7, IVDD C6/7, and space-occupying soft tissues ventral to this region. The radiographic findings might be compatible with osteomyelitis/discospondylitis, compression fracture, and soft tissue inflammation or hematoma. The bone tumor was less likely because of age and species. Post-mortem MRI of the cervicothoracic spine confirmed a shortened C7 vertebral body, a large amount of extradural material at C7 severely compressing the spinal cord from ventral and right sides, C6/7 discospondylopathy, and left-sided supra- and infraspinatus and longus coli muscles myopathy (Figure 11). These findings were consistent with a pathologic fracture of C7 and disc and probably bone material extrusion due to C6/7 discospondylitis.

Afterwards, a CT examination of the cervicothoracic part of the vertebral column was carried out for CT-guided tissue probing. Aggressive bone changes and compression fracture with the collapse of C7 were confirmed and were compatible with bacterial discospondylitis or abscess formation and a consequent pathologic fracture. CT-guided fine-needle aspiration (2×) from the C7 vertebral body confirmed acute, purulent discospondylitis and chondritis (Figure 12).

- Second group: In dead found animals, is it possible to detect the cause of death?

Clinical Question: What is the cause of death?

A total of 12 cases (12/20) were evaluated, and in 11 cases, virtopsy figured out the pathology leading to animal death compatible with the following necropsy studies.

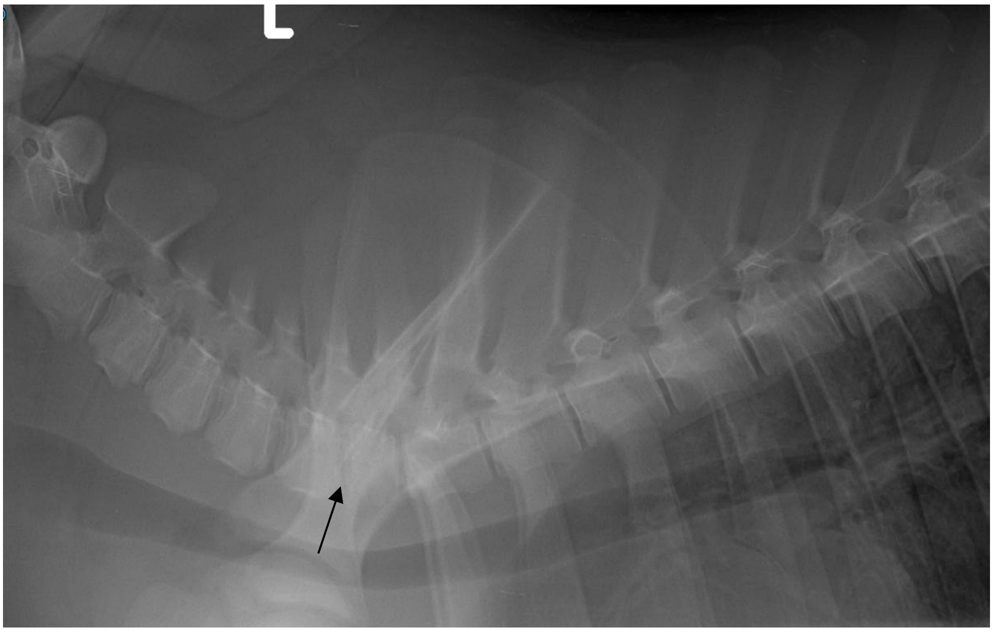

Figure 10. Lateral projection of a 7-month-old female pig in the region of cervical vertebra, C6/C7 intervertebral disc space, and C7 vertebral body is narrowed.

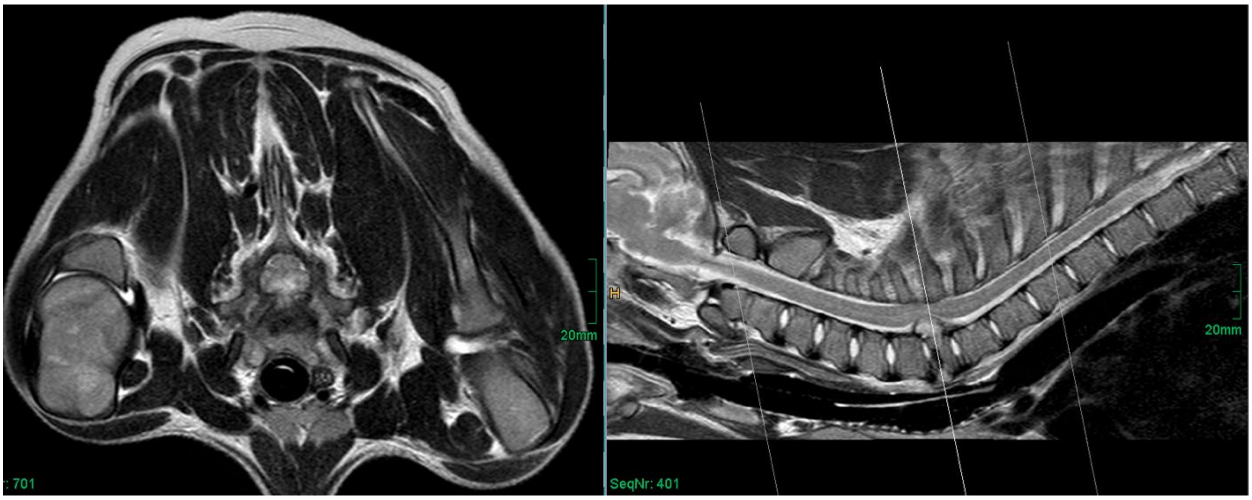

Figure 11. The same case as Fig 10: pathologic fracture of C7 and disc and probably bone material extrusion due to suspected C6/7 discospondylitis. The C6/7 intervertebral nucleus pulposus is smaller than the previous and following ones.

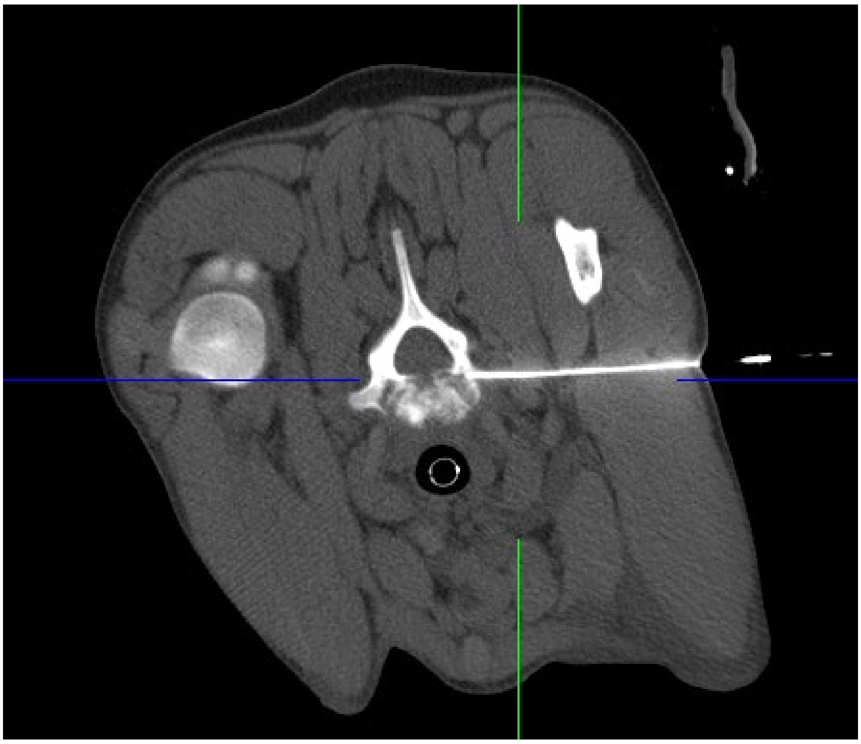

Figure 12. transverse image of the CT guided aspiration of C6 by a spinal needle.

Case no. 7

A skeletally immature female Eurasian lynx (Lynx lynx) was found dead. Lateral and dorsoventral radiographs of the skull and lateral views of the thorax and abdomen were taken. Several shrapnels associated with multi fragmented right mandible increased the opacity of the right tympanic bulla, and a small mineral opacity rostral to the odontoid process were detected (Figure 13). Some post-mortem changes were already visible, including lung atelectasis, intestinal functional ileus, and pneumobilia. Given the distribution of the shrapnels and the soft tissue swelling, the bullet trajectory could be from the caudodorsomedial aspect of the occiput to the right rostroventrolateral aspect to the right mandible.

Figure 13. orthogonal views of the skull of a female Eurasian lynx (Lynx lynx) showing the trajectory (arrows) of the gunshot shrapnels.

Case no. 8

A carcass of a bear was found, and the skull was studied by radiographs. Radiography revealed a metal bullet in the ventral aspect of the calvarium at the level of the left tympanic bullae and behind the left mandible (Figure 14). CT scan was performed later and identified multiple fractures in the midline of the frontal bone, indicating a gunshot trajectory through the skull, nasal cavity, ethmoidal bone, and left a perpendicular plate of the palatine bone. Bullet was visible in the soft tissue of the ventral aspect of the calvarium, the left lateral aspect of the trachea slightly behind the left mandible and Left TMJ, and slightly rostrally to the left tympanic bullae (Figure 15). The shrapnels could not be observed in the radiographs due to their small size and superimposition on the surrounding bones.

Figure 14. orthogonal radiographs of the skull of the bear with a metal bullet in the ventral aspect of the calvarium at the level of the tympanic left bulla and behind the left man-

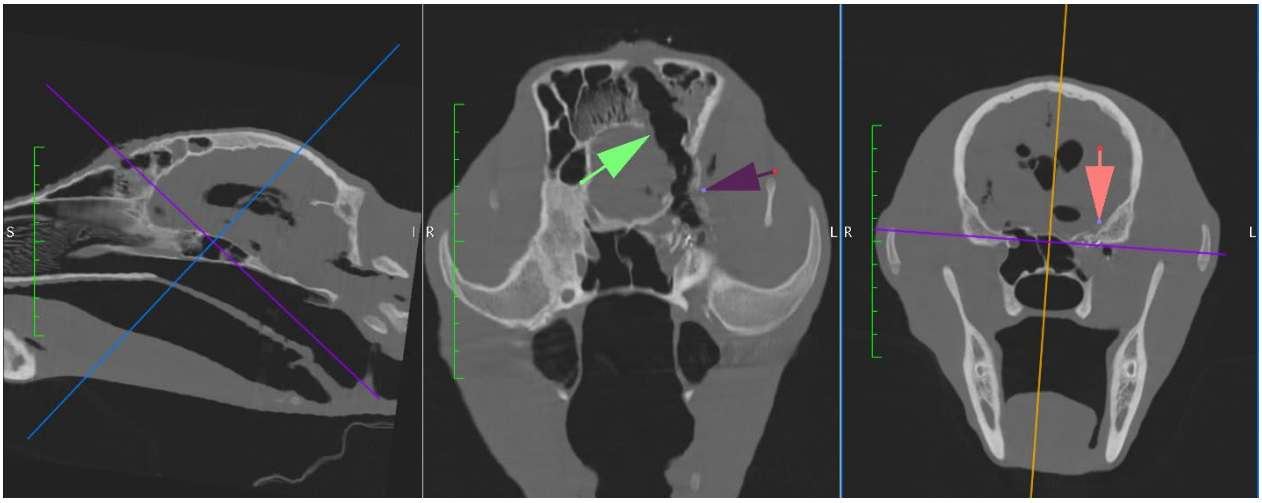

Figure 15. The same case as Figure 14: multiple fractures in the midline of the frontal bone indicating the gunshot trajectory through the skull, nasal cavity, ethmoidal bone, and left perpendicular plate of the palatine bone (arrows).

Cases no. 9 and 10

The corpse of two crows *(Corvus)* was found and presented to detect the reason for death. In case no 9, a metal density was visible at the right shoulder joint. In case 10, four bullets were found in the right humerus, left radius, right femur, and coelom cavity. Moreover, a transverse fracture at the tibiotarsal bone was visible, which could have resulted from falling on the ground after being shot (Figure 16).

Figure 16. Two crews with multiple gunshots.

Case no. 11

A female roe deer (Capreolus capreolus) was found dead. The post-mortem study consisted of one lateral view of the thorax, which included the caudal cervical region, almost the entire thorax, ventrocranial abdomen, entire right forelimb, and a part of the left forelimb (until the mid-3rd metacarpus). Luxation of the metacarpophalangeal joint of digits III and IV, right-sided subacute to chronic ossifying periostitis along the dorsal aspect of the right-sided 3rd metacarpus were found in the post-mortem radiographic study. Metallic structures confirming gunshot were not detected (Figure 17). Alveolar lung pattern associated with air bronchograms which are evidences of post-mortem lung lobe atelectasis are also noted.

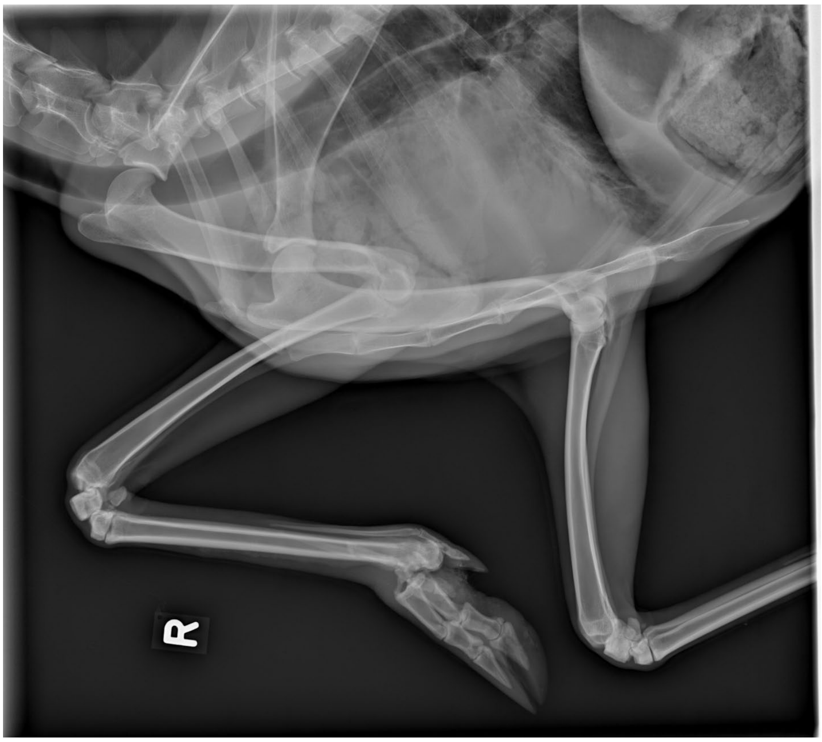

Figure 17. Luxation of the metacarpophalangeal joint of digit III and IV, right-sided and ill-defined smooth and solid periosteal reaction along the dorsal aspect of the right-sided 3rd metacarpus of a roe deer consistent with periostitis. Note the alveolar lung pattern with air-bronchograms.

Case no. 12

The carcass of a flamingo was found and referred to investigate the complications created in the legs and its connection with the death. Radiographic images of both legs were taken in the craniocaudal view. A complete spiral fracture was observed at the end of the left tibiotarsal bone. No metal density indicating a bullet was found (Figure 18).

Figure 18. A complete spiral fracture was observed at the end of the left tibiotarsal bone of a death flamingo.

Case no. 13

A cadaver of a 7-month-old female outdoor domestic shorthair cat was found dead by the owners in the yard and was referred for forensic investigations on the same day. In the whole-body CT scan, the right pleural cavity was filled with space-occupying hyperattenuating fluid which had displaced the mediastinum to the contralateral side. In addition, there was marked soft tissue swelling around the left forelimb associated with diffuse subcutaneous hyperattenuating lesions and multiple small gas inclusions. The skeletal structures were within normal limits. The changes were compatible with acute right-sided pleural hemorrhage, diffuse soft tissue swelling, and hemorrhage around the left forelimb which could be related to multicentric trauma (possibly cat biting) (Figures 19 and 20). In the necropsy, hemothorax due to a small perforating trauma was concluded.

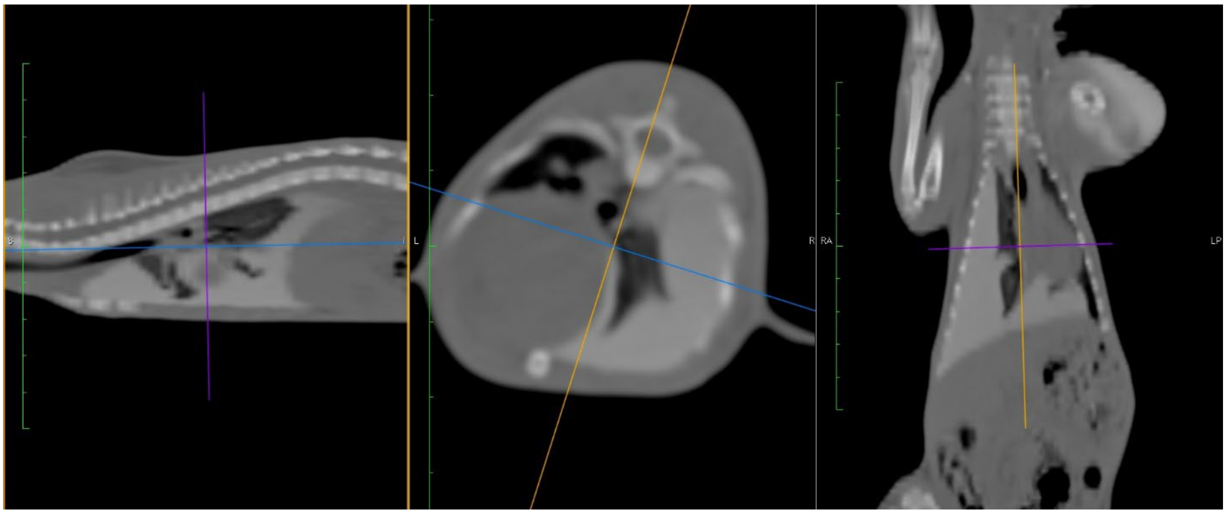

Figure 19. Almost immediate post-mortem image of a 7-month-old female outdoor domestic shorthair cat with right-sided pleural hemorrhage.

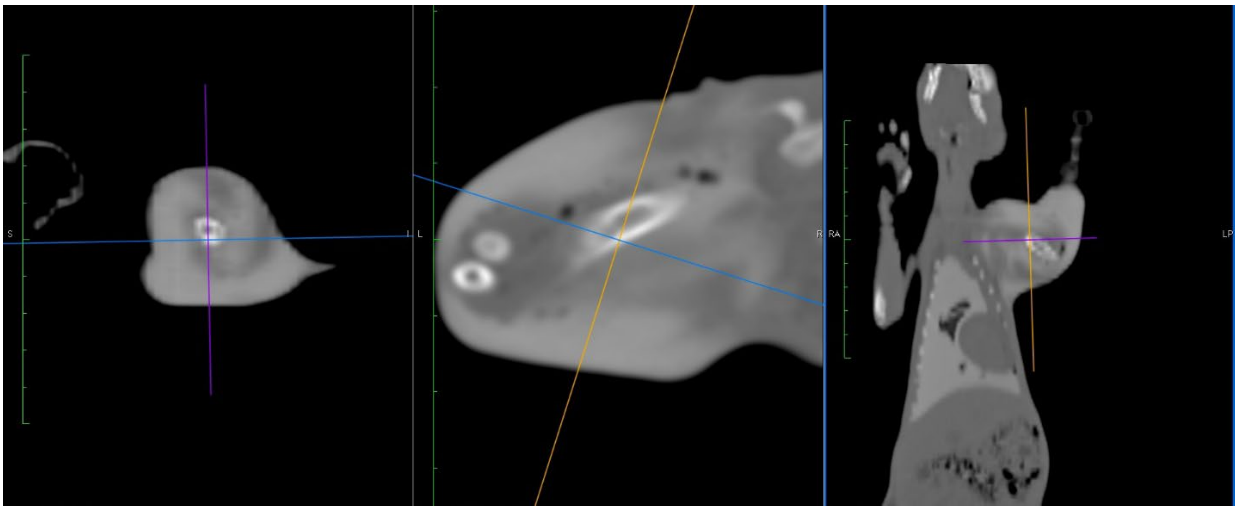

Figure 20. Almost immediate post-mortem image of the same case as Fig 19 with soft tissue swelling and hemorrhage around the left forelimb.

Case no. 14

The cadaver of a 6-year-old Jack Russell Terrier male dog was presented for forensic studies. Initially, a post-mortem CT scan of the whole body revealed multiple fractures on the right zygomatic arch, lateral wall of the occipital condyle, atlas, axis, and C4 with multiple gas inclusions in the soft tissues on the right lateral side of the skull and extensive soft tissue lacerations on the right lateral side of the neck. The right eye globe and lens were deformed. The urinary bladder wall was noticeably thickened and only a little inhomogeneous content with small gas pockets in the urinary bladder was visible. It was observed that a soft tissue density (intervertebral disc, dorsal and ventral intervertebral ligament) protruded on the lumbosacral junction.

Post-mortem MRI of the skull and cervical spine was performed to evaluate probable brain and spinal cord damages. Large skin lacerations at the level of C2-C6 with lacerations and interruption of the spinal cord at C1 and C2/3 were noted. Moreover, we detected multiple fractures of the right parietal bone and the skull base with marked compression and dislocation along with moderate destruction of the right brain hemisphere and adjacent soft tissue associated with several hemorrhagic lesions and gas inclusion. Based on the signal characteristics of the visible hemorrhages, acute bleeding was suspected (T1w iso, T2w hyperintense with T2* susceptibility artifact). The findings indicated a possible trauma to the head and neck and no evidence of metal fragments that suggest bullets (Watson *et al.*, 2017). The shape of the wounds associated with the depression fractures was speaking of trauma by a blunt instrument (e.g., hammer) (Watson *et al.*, 2017; Benetato *et al.*, 2011) (Figures 21 and 22).

Figure 21. Three-dimensional rendering image of a 6-year-old Jack Russell Terrier with a skull compression fracture.

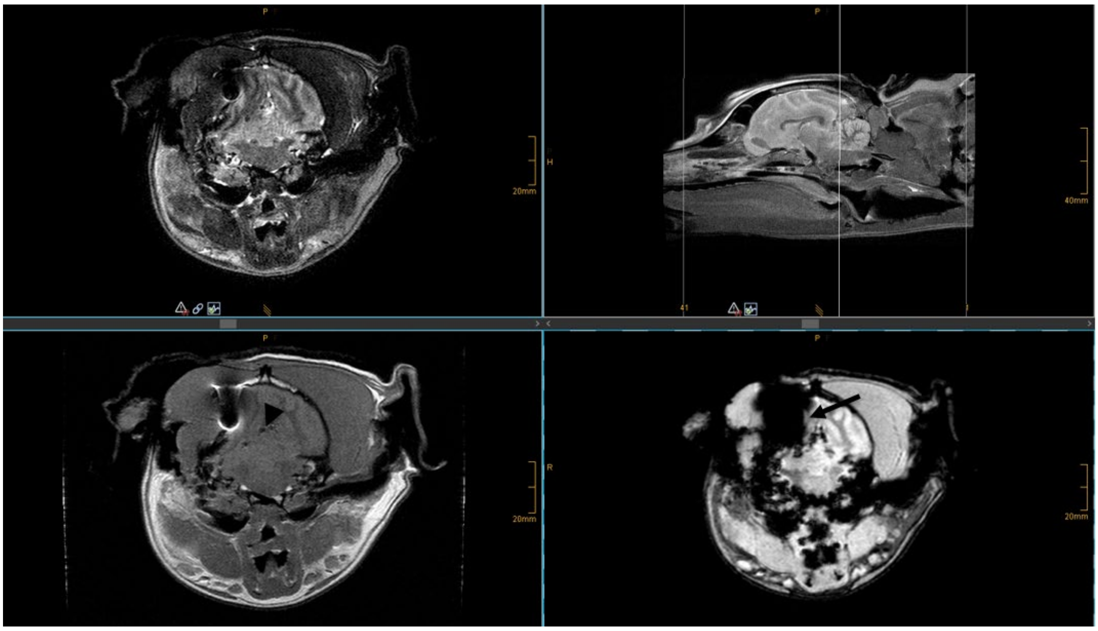

Figure 22. Transverse T1w, T2w, and T2* and a sagittal T2w showing several hemorrhagic lesions (arrow) and gas inclusion (arrowhead) in the left temporal aspect of the skull and the cerebrum.

Case no. 15

A skeletally mature Persian male cheetah was referred for forensic assessment two days after an acute longitudinal L5 fracture open reduction and stabilization by internal fixation. Post-mortem radiography and CT scan were performed to find out the reason for death. A severely displaced L5 and minimally displaced T8 fractures associated with implant failure and additional small fragments of L5 compared to the pre-operative radiographs were detected. In addition, abdominal effusion, solitary cavitary lung lesion, and megaesophagus with some food material were visible. The abdominal effusion aspirated under ultrasound guidance and acute abdominal hemorrhage was found. The cavitary lung lesions were indicative of traumatic lung bulla and the esophageal changes were most likely post-mortem changes. Implant failure creating hemorrhage was considered the main reason for death (Figures 23 and 24).

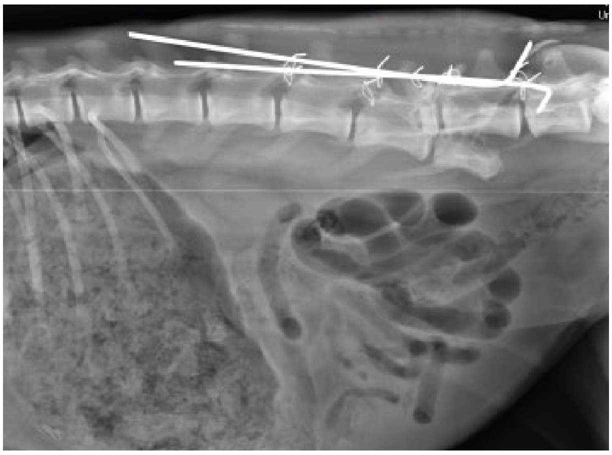

Figure 23. Lateral radiograph of the lumbar spine of a Persian Cheetah with implant failure and severely displaced L5 fracture.

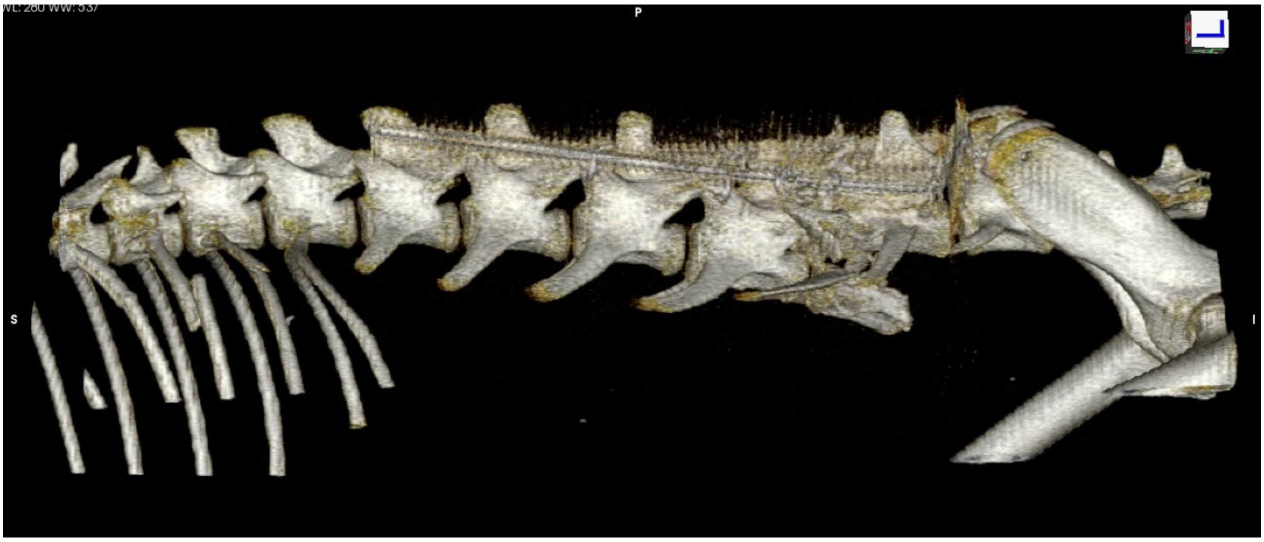

Figure 24. Three-dimensional rendering reconstructed images of the lumbar spine of a Persian Cheetah with implant failure and severely displaced L5 fracture.

Case no. 16

An 11-year-old female herd guard dog was found dead, and the carcass was presented to detect the cause of death. Severe post-mortem autolysis developed prior to the post-mortem examination. Whole-body post-mortem CT scan revealed bilateral moderate to severe osteoarthritis in the stifle joints with the signs of joint effusion with the Hounsfield Unit of 45 (Figure 25) compatible with erosive arthritis (e.g., rheumatoid, immune-mediated, leishmaniosis), lesion of the cranial cruciate ligament, or primary osteoarthritis. There was a bilateral partial obstruction of the external ear canal by soft tissue attenuating material (Figure 26) which might be due to chronic otitis externa or neoplastic process (ceruminoma). The findings could not explain the main reason for death in this case. Necropsy also failed to find the main fetal pathology.

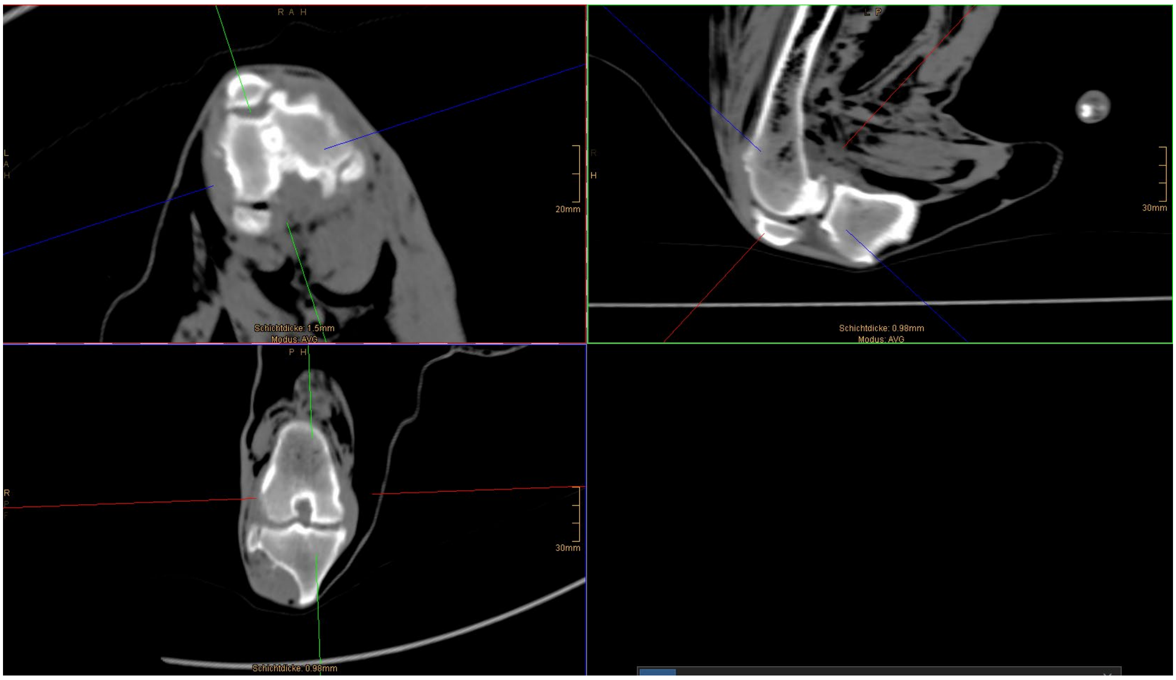

Figure 25. Orthogonal CT scan reconstructed images of the right stifle joint of a dead female herd guard dog with moderate degenerative or inflammatory osteoarthritis.

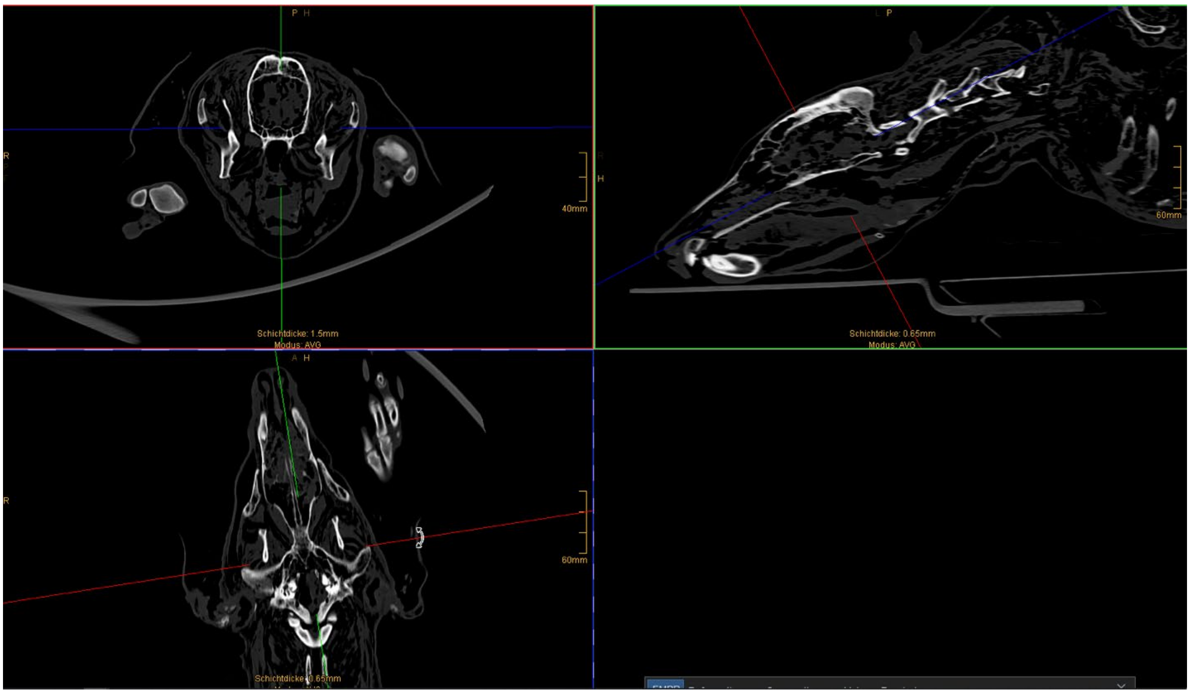

Figure 26. Orthogonal CT scan of the skull of the same dog as Fig 25 with severe post mortem putrefaction.

Case no. 17

The body of a skeletally mature European short-hair female cat was presented for necropsy. Post-mortem radiography and CT scan of the whole body revealed patchy hyper densities in both nasal cavities

(L>R), hyperdense material in the lateral compartment of the left bulla, subcutaneous and connective gas inclusions in the region of the pharynx, neck, and the thoracic wall along the trachea and esophagus, pneumomediastinum, connecting severe bilateral pneumothorax, and subluxation of the left stifle joint with a ruptured cranial cruciate ligament. There was a defect in the dorsal aspect of the trachea in its most cranial part (Figures 27 and 28). No signs of skin lacerations were observed. Therefore, tracheal rupture might have been due to blunt trauma or the passage of a traumatic material through the esophagus.

Figure 27. Lateral view of the skull of a European shorthair female cat with retropharyngeal and subcutaneous emphysema and pneumomediastinum.

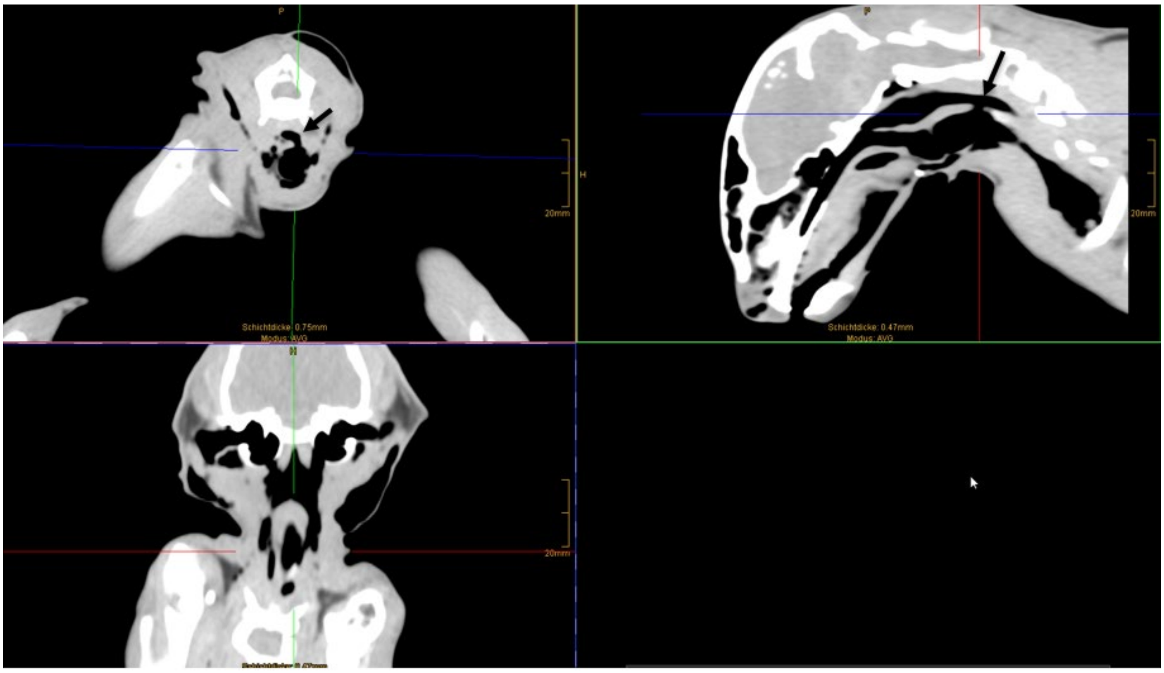

Figure 28. Three planar reconstructed images of the cat's skull as shown in Figure 27, with a defect visible in the dorsal wall of the proximal trachea (arrow) associated with large amounts of surrounded emphysema.

Case no. 18

A 12-year-old Californian sea lion *(Zalophus californianus)* was found dead without prior significant clinical signs. Primary full-body radiography showed a metal density superimposed on the intestinal lumen. A post-mortem CT scan confirmed the presence of one irregular linear metallic foreign body in the stomach associated with small amounts of pneumoperitoneum with peritoneal effusion. These findings were compatible with a perforating foreign body causing infectious peritonitis confirmed later by necropsy (Figures 29 and 30).

The most common indication for the referral cases of death with unknown cause was being shot by a gun (Table 1).

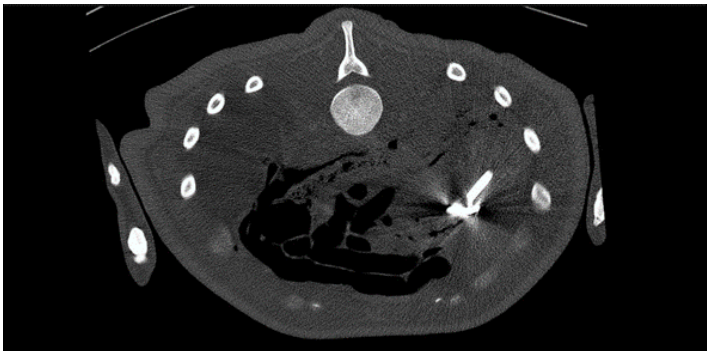

Figure 29. Transverse CT images of the abdomen of a dead Californian sea lion with 2 metallic foreign body segments in the gastric body, the ventromedial one in the pyloric antrum is perforated. There is a moderate amount of gas in the peritoneal and retroperitoneal regions.

Figure 30. Dorsoventral radiograph of the same case as shown in Figure 29 with an irregular linear metallic foreign body superimposed on the intestinal loops.

Table 1. Virtopsy of death causes by type of pathology.

number	Species (genus)	Imaging modality by time order (part)	Sampling	Age	Imaging modality by time order (part)	Sampling	Final Diagnosis	Type of the pathology
1	Dog/F	Rad (WB) CT (WB)	CT-guided biopsy	7 ys	Rad (WB) CT (WB)	CT-guided biopsy	Neoplastic	osteosarcoma
2	Cat/M	MRI (WB) CT(WB)	US-guided biopsy	11 ys	MRI (WB) CT(WB)	US-guided biopsy	Neoplastic	Mast cell carcinoma
3	Cat/F	Rad (thorax) MRI (spine) US (abdomen)	US-guided FNA	16 ys	Rad (thorax) MRI (spine) US (abdomen)	US-guided FNA	Neoplastic	Lymphoma
4	African grey parrot/U	Rad (WB) CT (skull)	US-guided FNA	-	Rad (WB) CT (skull)	US-guided FNA	Infectious	Abscess
5	Dog/M	Rad (stifle)	US-guided biopsy	12 ys	Rad (stifle)	US-guided biopsy	Infectious	Lishmaniosis
6	Pig/F	Rad (spine). CT (spine). MRI (spine)	US - guided biopsy	7 ms	Rad (spine). CT (spine). MRI (spine)	US - guided biopsy	Infectious	Purolent discospondylistis
7	Eurasian lynx/M	Rad (WB)	-	Skeletally immature	Rad (WB)	-	Trauma	Gunshot
8	Bear/F	Rad (skull) CT (skull)	-	Skeletally mature	Rad (skull) CT (skull)	-	Trauma	Gunshot
9	Crow/U	Rad (WB)	-	-	Rad (WB)	-	Trauma	Gunshot
10	Crow/U	Rad (WB)	-	-	Rad (WB)	-	Trauma	Gunshot
11	Roe deer/F	Rad (forelimbs)	-	Skeletally mature	Rad (forelimbs)	-	Trauma	Chronic luxation
12	Flamingo/U	Rad (legs)	-	-	Rad (legs)	-	Trauma	Acute fracture
13	Cat/F	CT (WB)	US-guided	7ms	CT (WB)	US-guided	Trauma	Bite

numbe r	Species (genus)	Imaging modality by time order (part)	Samplin g	Age	Imaging modality by time order (part)	Samplin g	Final Di-agnosis	Type of the pathology
			aspiratio n			aspiratio n		
14	Dog/M	CT (skull) MRI (skull)	-	6ys	CT (skull) MRI (skull)	-	Trauma	Blunt hard device
15	Persian Cheetah/F	Rad (WB) CT (WB)	necropsy	Skeletall y mature	Rad (WB) CT (WB)	necropsy	Iatrogenic	Implant failure
16	Dog/F	CT (WB)	necropsy	11 ys	CT (WB)	necropsy	-	-
17	Cat/M	Rad (WB) CT (WB)	necropsy	Skeletall y mature	Rad (WB) CT (WB)	necropsy	Hallow organ rupture	Tracheal perfuration
18	California Sealion/U	Rad (WB) CT(WB)	necropsy	12 ys	Rad (WB) CT(WB)	necropsy	Hallow organ rupture	Perforating foreign body
19	Mammifie d fetus (Calf)	Rad	-	-	Rad	-	Congenit al	Bullgod calf syndrome
20	Covered box	Rad	-	-	Rad	-	-	Canine bones

- <u>Third group: in the case of bog bodies, is it possible to identify the animal and the probable cause of death?</u>

Question: Which kind of animal species?

Case no. 19

A mummified animal carcass was found and sent as a possible wolf or lynx. Post-mortem orthogonal view radiographs of the whole body were taken with severe abnormal positions due to the rigidity of the dead body. The body and limbs were shortened and compressed due to the reduced length of the spine and long bones, while the head was markedly enlarged compared to the rest of the body. The appendicular skeleton was grossly deformed. The distal parts of the limbs deviated bilaterally and symmetrically, with two digits in the distal limbs. The face showed severe dysplasia. The calvarium was prominent and dome-shaped, with an almost 90° angular ventral deviation of the facial bones to the axis of the brain. The frontal and occipital bones were thick, and the fontanel was wide.

The mandible and maxilla were the most developed structures with severe pragmatism. Mandibular incisors, premolars, and molars were present. Maxillary incisors and canine teeth were absent. The premolar and molars were severely crowded due to the skull deformity. The dorsal border of the nasal bone had a "bullterrier-like" convex shape. Nasal and ethmoid turbinate bones were present with heterogeneous parenchyma.

The spine and long bones of the limbs showed severe dysplastic features. Their diaphysis was small and misshapen with diffusely increased opacity, and the tibiae and tarsal bones were significantly thickened. The metacarpal and metatarsal bones were severely shortened and the digits are not formed completely. The vertebrae were compressed, and the right and left parts of the dorsal spinous processes of the thoracic and lumbar spine widely failed to fuse. Some ribs were present with cranial orientation. The thorax and abdomen volume was reduced, and the enclosed organs were not delineated. The radiographic appearance of the generalized congenital chondrodysplasia associated with the absence of the maxillary incisors and canine teeth and the presence of two distal phalanxes in the limbs were in favor of a ruminant. The deformities of the skull and limb conformation resemble changes observed in "bulldog calf syndrome" (Watson *et al.*, 2017) (Figure 31).

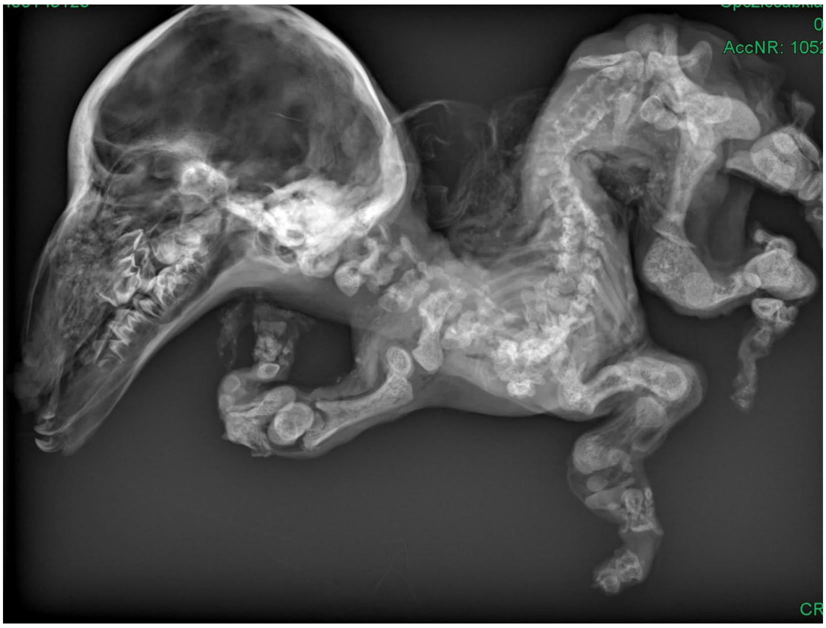

Figure 31. A lateral radiograph of a weird mummified animal carcass with shortened and compressed limbs, small, misshapen vertebral bodies, and markedly disproportional enlarged skull compared to the rest of the body.

Case no. 20

A box of bones was submitted to search for projectiles, fractures, or other trauma. In order to prevent the potential loss of a projectile or other important forensic materials, the bag could not be opened. Multiple mature bones with associated soft tissues and multiple gas inclusions were randomly distributed. A normal body conformation was not visible. No obvious fractures were identified; instead, multiple joints were completely luxated. Both mandibular rami were separated from the rest of the skull and maxilla. Only a short vertebral segment with three completely misshapen and shrunk vertebral segments and an additional subluxated one were visible. A few coccygeal vertebrae were identified, while scapulae were not visible. One independent humerus and another humerus with an associated radius/ulna and carpus/manus were visible. An additional radius/ulna was also found without associated carpus/manus. The hip was separated from the sacrum and femora. Subluxation of one stifle and ipsilateral tarsus/foot and the complete separation of the other stifle and tarsus/phalanges were notable. Two elongated metal opaque structures are partially superimposed on the animal. No metallic bullets or fractured bones were found. Based on the shape of the skeletal structures and closed growth plates, in addition to several luxations, a skeletally matured canine species was the final answer (Figure 32).

Figure 32. Radiology of a bag of bones without identification.

Discussion

Radiography has been used frequently in veterinary virtopsy (Thali *et al.*, 2007; Cooper *et al.*, 2008; Ibrahim *et al.*, 2012; Wolosker *et al.*, 2021). Serial post-mortem imaging of the thorax and abdomen in dogs and post-mortem radiographic findings in the abdomen of cats have been described (Cooper *et al.*, 2008; Heng *et al.*, 2009; Cavard *et al.*, 2011; Ibrahim *et al.*, 2012; Hamano *et al.*, 2014; Wolosker *et al.*, 2021). Post-mortem imaging of projectile trauma in wildlife is also performed routinely (Thali *et al.*, 2007; Heng *et al.*, 2008). Post-mortem CT imaging confirmed sudden death due to skull trauma in caged layer chickens by a moving feeder hopper (Morrow *et al.*, 2012). There are few reports of post-mortem evidence-based cross-sectional imaging for finding the cause of death in the veterinary literature (Thali *et al.*, 2007; Hamano *et al.*, 2014; Hostettler *et al.*, 2015). Post-mortem CT-guided biopsy was described in Bernese mountain dogs with suspected histiocytic (Hostettler *et al.*, 2015). Histiocytic sarcoma was confirmed in 10 of 11 dogs by this technique. Two reports of the post-mortem imaging of exotic animals leading to final diagnoses have also been published (Hamano *et al.*, 2014; Gascho *et al.*, 2020).

In our series, the post-mortem protocols included 11 whole body and partial CT scans and four partial MRI examinations, which is unique in terms of the number. The CT scan and MRI are described to be valuable imaging modalities for noninvasive necropsy in animals (Watson *et al.*, 2017). These techniques have been performed to examine a gravid Boa and confirm fetal death (Gascho *et al.*, 2020). Moreover, virtopsy allowed chronological age estimation by the degree of epiphyseal ossification and closure as well as bone mineral density evaluation by quantitative CT, both of which may contribute to the assessment of biological health.

In our study, virtopsy was successful in detecting three neoplastic and three infection antemortem pathologies out of six referred cadavers which can open a horizon in post-mortem veterinary clinical investigations. Based on the modality selection, in five cases, plain radiology was the first modality of choice, followed by MRI, CT scan, and/or ultrasonography based on the radiographic findings. Our results also showed that in a series of unselected deaths, there was a discrepancy between autopsy and imaging causes of death in 91.7% of cases. Overall, radiology was the most used modality. The most common reason for the death of unknown causes was being shot with a gun and trauma, which were unique in our case series. This is in line with the other studies, which discussed the importance of virtopsy in evaluating gunshot injuries (Benetato *et al.*, 2011; Watson *et al.*, 2017). Virtopsy has also been mentioned as the most accurate means of forensic veterinary analysis of gunshot wounds in animals (Watson *et al.*, 2017). The identification of wired and bizarre cadavers is occasionally involved in forensic investigations. If there is a suspicion of human body remnants, clinic-legal examinations are required. However, these containers are occasionally locked (Watson *et al.*, 2017). Commuted tomography can reveal the content of a highly radiopaque forensic Pandora's Box successfully (Gascho *et al.*, 2018). In the present study, radiology could present the contents of such strange corpses.

In general, we recommend the following guideline in daily veterinary practice:

- Get a clear history by forensic, clinical, or legal question(s),

- Take plain radiographs from the whole body and try to find the general aspect of the cadaver (i.e., dry bones, mummified body, fragmented, putrefied, intact, and carbonized), body conformation, and the proportion of organs compared to the axial skeleton,

- Investigate the skeletal structure to find age, spices, and gender if possible,

- If the radiographs could not address the questions, choose cross-sectional imaging, followed by an ultrasound-guided sampling of the suspicious lesions.

Post-mortem imaging in veterinary practice has a clear advantage compared to clinical imaging such as the absence of motion artifacts. Otherwise it has some major problems like the inability to perform the standard projections. However, a couple of publications describing using polyethylene glycol iodinated contrast medium have been recently released (Wolosker *et al.*, 2021; Gascho *et al.*, 2018).

Conclusion

The case series in our “"irtopsy”"project demonstrated that diagnostic imaging techniques are feasible in answering different clinical antemortem and post-mortem clinical and forensic questions. However, there is an interdisciplinary collaboration between diagnostic imaging and sampling under imaging guidance. In addition, the current study was the first to provide SOP guidelines in veterinary virtopsy to reduce the time, manage the quality, and facilitate the entire workflow more effectively and efficiently.

Acknowledgments

The authors appreciate the efforts of Dr. Iman Memariyan (Chief Veterinarian of Tehran zoo and Pardisan Rehabilitation Centre).

Conflict of Interest

The authors declared no conflict of interests.

References

Buck, U., Christe, A., Naether, S., Ross, S., & Thali, M. J. (2009). Virtopsy—noninvasive detection of occult bone lesions in post-mortem MRI: additional information for traffic accident reconstruction. *International Journal of Legal Medicine*, *123*(3), 221-226. [DOI:10.1007/s00414-008-0296-5] [PMID]

Cavard, S., Alvarez, J. C., De Mazancourt, P., Tilotta, F., Brousseau, P., de la Grandmaison, G. L., & Charlier, P. (2011). Forensic and police identification of “X” bodies. A 6-years French experience. *Forensic Science International*, *204*(1-3), 139-143. [DOI:10.1016/j.forsciint.2010.05.022] [PMID]

Delannoy, Y., Becart, A., Colard, T., Delille, R., Tournel, G., Hedouin, V., & Gosset, D. (2012). Skull wounds linked with blunt trauma (hammer example). A report of two depressed skull fractures–Elements of biomechanical explanation. *Legal Medicine*, *14*(5), 258-262. [DOI:10.1016/j.legalmed.2012.04.006] [PMID]

Gascho, D., Bolliger, S. A., Enders, M., Thali, M. J., & Fliss, B. (2018). Pandora’s box. *Forensic Science, Medicine and Pathology*, *14*(1), 120-122. [DOI:10.1007/s12024-018-9948-z] [PMID]

Gascho, D., Hetzel, U., Schmid, N., Martinez, R. M., Thali, M. J., & Richter, H. (2020). Virtopsy of a gravid

Boa constrictor using computed tomography and magnetic resonance imaging. *Veterinary and Animal Science*, *10*, 100150. [DOI:10.1016/j.vas.2020.100150] [PMID] [PMCID]

Hamano, T., Terasawa, F., Tachikawa, Y., Murai, A., Mori, T., El-Dakhly, K., ... & Yanai, T. (2014). Squamous cell carcinoma in a capybara (Hydrochoerus hydrochaeris). *Journal of Veterinary Medical Science*, *76*(9), 1301-1304. [DOI:10.1292/jvms.13-0395] [PMID] [PMCID]

Heng, H. G., Teoh, W. T., & SHEIKH-OMAR, A. R. (2008). Postmortem abdominal radiographic findings in feline cadavers. *Veterinary Radiology & Ultrasound*, *49*(1), 26-29. [DOI:10.1111/j.1740-8261.2007.00312.x] [PMID]

Hostettler, F. C., Wiener, D. J., Welle, M. M., Posthaus, H., & Geissbühler, U. (2015). Post mortem computed tomography and core needle biopsy in comparison to autopsy in eleven bernese mountain dogs with histiocytic sarcoma. *BMC Veterinary Research*, *11*(1), 1-11. [DOI:10.1186/s12917-015-0544-0] [PMID] [PMCID]

Ibrahim, A. O., Zuki, A. B. M., & Noordin, M. M. (2012). Applicability of virtopsy in veterinary practice: a short review. *Pertanika Journal of Tropical Agricultural Science*, *35*(1), 1-8.

Morrow, C. J., Noormohammadi, A. H., & O'Donnell, C. J. (2012). Fatal skull trauma in caged layer chickens associated with a moving feed hopper: diagnosis based on autopsy examination, forensic computed tomography and farm visit. *Avian Pathology*, *41*(4), 391-394. [DOI:10.1080/03079457.2012.697126] [PMID]

Pewsner, M., Origgi, F. C., Frey, J., & Ryser-Degiorgis, M. P. (2017). Assessing fifty years of general health surveillance of roe deer in Switzerland: a retrospective analysis of necropsy reports. *PloS One*, *12*(1), e0170338. [DOI:10.1371/journal.pone.0170338] [PMID] [PMCID]

Thali, M. J., Kneubuehl, B. P., Bolliger, S. A., Christe, A., Koenigsdorfer, U., Ozdoba, C., ... & Dirnhofer, R. (2007). Forensic veterinary radiology: ballistic-radiological 3D computertomographic reconstruction of an illegal lynx shooting in Switzerland. *Forensic Science International*, *171*(1), 63-66. [DOI:10.1016/j.forsciint.2006.05.044] [PMID]

Thali, M., Dirnhofer, R., & Vock, P. (2009). The virtopsy approach: 3D optical and radiological scanning and reconstruction in forensic medicine. CRC Press. [DOI:10.1201/9780849381898]

Thali, M. J., Viner, M. D., & Brogdon, B. G. (Eds.). (2010). *Brogdon's Forensic Radiology*. CRC press. [DOI:10.4324/9780367805708]

Watson, E., & Heng, H. G. (2017). Forensic radiology and imaging for veterinary radiologists. *Veterinary Radiology & Ultrasound*, *58*(3), 245-258. [DOI:10.1111/vru.12484] [PMID]

Wolosker, M. B., Leiderman, D. B. D., Estevan, F. A., Wolosker, N., Zerati, A. E., & Amaro Jr, E. (2021). Comparative Analysis of Artery Anatomy Evaluated by Postmortem Tomography, CT Angiography, and Postmortem and Predeath CT Scans. *Annals of Vascular Surgery*, *72*, 124-137. [DOI:10.1016/j.avsg.2020.09.005] [PMID].

10.22059/IJVM.2022.331329.1005197

Iranian Journal of Veterinary Medicine

Abstracts in Persian Language

Online ISSN 2252-0554

مجله طب دامی ایران، ۱۴۰۱، دوره ۱۶، شماره ۳، ۳۱۱-۳۳۶

امکان سنجی استفاده از ویرتوپسی مبتنی بر شواهد برای پاسخ به سؤالات احتمالی بالینی و پس از مرگ، در دامپزشکی

محمد ملازم[1,2]، ارزو رمضانی[1]، سارنگ سروری[1]، زهرا جعفری گیو[1]، سارا شکرپور[3]، اورس گیسبوهلر[2]

[1]گروه جراحی و رادیولوژی، دانشکده دامپزشکی، دانشگاه تهران، تهران، ایران

[2]گروه دامپزشکی بالینی، بخش رادیولوژی بالینی، دانشکده Vetsuisse برن، دانشگاه برن، برن، سوئیس

[3]. گروه پاتولوژی، دانشکده دامپزشکی، دانشگاه تهران، تهران، ایران

(دریافت مقاله: 13 دی ماه 1400، پذیرش نهایی: 23 اسفند 1400)

معاینه پس از مرگ بخش مهمی در پزشکی مبتنی بر شواهد برای درک بدتر شدن علائم بالینی یا علل مرگ در حیوانات یا حتی جمعیت‌های کشته‌شده یا مرده است.

هدف از تجزیه و تحلیل پس از مرگ، بهبود درمان و درمان بالینی، تأیید تشخیص های مورد شک، مدیریت استراتژی‌های اصلاح نژاد یا روشن کردن شرایطی است که منجر به مرگ در موارد پزشکی قانونی شده است. در قیاس با ویرتوپسی در پزشکی انسانی، روش‌های تصویربرداری تشخیصی در دامپزشکی پس از مرگ که ما آن را Vetvirtopsy می‌نامیم، استفاده شده‌است.

ما فرض می‌کنیم که Vetvirtopsy می‌تواند به‌عنوان روشی برای سؤالات بالینی/پس از مرگ خاص برای افزایش اطمینان تشخیص استفاده شود. در برخی سوالات، Vetvirtopsy در واقع می‌تواند جایگزین کالبدگشایی معمولی شود. هدف از این مطالعه مرور مقایسه ای Vetvirtopsy با کالبدگشایی معمولی در علل متغیر مرگ و میر در حیوانات و تعریف امکانات و محدودیت‌های آن است.

بدین منظور حیوانات خانگی مرده یا معدوم شده و حیوانات وحشی جمع‌آوری شدند. روش‌های مورد استفاده تکنیک‌های تصویربرداری مانند رادیوگرافی دیجیتال پس از مرگ، سونوگرافی پس از مرگ، توموگرافی کامپیوتری پس از مرگ و توموگرافی تشدید مغناطیسی پس از مرگ در ترکیب با نمونه‌برداری بافت (هدایت‌شده با تصویر) برای پاسخگویی به سؤالات باز در مورد علائم بالینی یا علل مرگ آنها هستند .

مجموعه موارد این مطالعه نشان داد که استفاده از تکنیک تصویربرداری تشخیصی در پاسخ به سوالات مختلف بالینی پیش و پس از مرگ و پزشکی قانونی امکان پذیر است.

واژه‌های کلیدی: ویرتوپسی ، رادیوگرافی ، سونوگرافی ، توموگرافی کامپیوتری ، توموگرافی رزونانس مغناطیسی

نویسندهٔ مسئول: محمد ملازم، گروه جراحی و رادیولوژی، دانشکده دامپزشکی، دانشگاه تهران، تهران، ایران ایمیل:Mmolazem@ut.ac.ir